Published in "Spectrochimica Acta Part A: Molecular and Biomolecular Spectroscopy doi: 10.1016/j.saa.2020.118416, 2020" which should be cited to refer to this work.

Indirect solvent assisted tautomerism in 4-substituted phthalimide 2-hydroxy-Schiff bases

Dancho Yordanov [a], Vera Deneva [a], Anton Georgiev [b,c,*], Aurelien Crochet [d], Katharina M. Fromm [d], Liudmil Antonov [a,e,**]

[a] Institute of Organic Chemistry with Centre of Phytochemistry, Bulgarian Academy of Sciences, 1113 Sofia, Bulgaria
[b] Department of Organic Chemistry, University of Chemical Technology and Metallurgy, 1756 Sofia, Bulgaria
[c] Institute of Optical Materials and Technologies, Bulgarian Academy of Sciences, 1113 Sofia, Bulgaria
[d] Department of Chemistry and Fribourg Center for Nanomaterials FriMat, University of Fribourg, CH-1700 Fribourg, Switzerland
[e] Institute of Electronics, Bulgarian Academy of Sciences, 1784 Sofia, Bulgaria

Keywords:
ESIPT
Phthalimides
2-hydroxy-Schiff bases
Enol/keto tautomerism
Phototautomerization
DFT
UV–Vis spectroscopy
Crystallography

The paper presents the synthesis and characterization of two 4-substituted phthalimide 2-hydroxy-Schiff bases containing salicylic (**4**) and 2-hydroxy-1-naphthyl (**5**) moieties. The structural differences of 2-hydroxyaryl substituents, resulting in different *enol*/*keto* tautomeric behaviour, depending on the solvent environment were studied by absorption UV–Vis spectroscopy. Compound **5** is characterized by a solvent-dependent tautomeric equilibrium (K_T in toluene = 0.12, acetonitrile = 0.22 and MeOH = 0.63) while no tautomerism is observed in **4**. Ground state theoretical DFT calculations by using continuum solvation in MeOH indicate an energy barrier between *enol*/*keto* tautomer 5.6 kcal mol^{-1} of **4** and 0.63 kcal mol^{-1} of **5**, which confirms the experimentally observed impossibility of the tautomeric equilibrium in the former. The experimentally observed specific solvent effect in methanol is modeled via explicit solvation.
The excited state intramolecular proton transfer (ESIPT) was investigated by steady state fluorescence spectroscopy. Both compounds show a high rate of photoconversion to *keto* tautomers hence *keto* emissions with large Stokes shifts in five alcohols (MeOH, EtOH, 1-propanol, 1-butanol, and 1-pentanol) and various aprotic solvents (toluene, dichlormethane, acetone, AcCN). According to the excited state TDDFT calculations using implicit solvation in MeOH, it was found that *enol* tautomers of **4** and **5** are higher in energy compared to the *keto* ones, which explains the origin of the experimentally observed *keto* form emission.

1. Introduction

The aromatic 2-hydroxy substituted Schiff bases (SB's), able to undergo solvent-assisted or photoinduced *enol*/*keto* tautomerization via excited state intramolecular proton transfer (ESIPT) [1–3], are of substantial scientific interest. The ESIPT phenomenon finds potential applicability in the development of metal ions sensors, proton based photoswitches, light driven molecular motors, molecular logic gates, OLED's and solar cell fabrication, labeling cell image biology and others [4–13]. There are a large number of synthesized and investigated 2-hydroxy substituted SB's and other derivatives by intramolecular hydrogen HHO bonding with multifarious structures – from 2-hydroxyazo and azomethine chromophores to differently substituted pyridines, pyrazoles, coumarins, quinolones, isoquinolines, etc. [1,3].

Depending on the electronic effects of 2-hydroxyaryl substituents, the tautomerization –O–H·····N≤ ⇋ =O·····HN < in SB's could be triggered by solvents or photoexcitation. Several factors influence the process: (i) the –O-H acidity of 2-hydroxyaryl substituents enable hydrogen bonding with azomethine nitrogen resulting in *enol*/*keto* equilibrium. The conjugated *keto* base is stabilized by π-π delocalization with the aryl moiety by increasing the number of rings or by introducing the electron withdrawing (EW) substituents resulting in a shifted equilibrium toward the *keto* form [3,14–18]; (ii) the basicity (nucleophilicity) of:N ≤ azomethine by a nonbonding electron pair to form a conjugate acid. The key factor here is the Ar–CH=N − Ar^2 ⇋ Ar = CH − HN − Ar^2 rearrangement by proton transfer reaction, where the π-motion is favored by the stability of *keto* form and by donor-acceptor interactions in –NH–Ar^2 moiety. The electron donating (ED) groups increase the basicity of nitrogen atom able to form a conjugated –NH-Ar^2 acid. On the other hand, EW groups cause n-π conjugation,

* Correspondence to: A. Georgiev, University of Chemical Technology and Metallurgy, 1756 Sofia, Bulgaria.
** Correspondence to: L. Antonov, Bulgarian Academy of Sciences, Sofia, Bulgaria
E-mail addresses: antonchem@abv.bg (A. Georgiev), lantonov@orgchm.bas.bg,
URL: http://www.tautomer.eu (L. Antonov).

which is increased after the protonation of nitrogen; (iii) the solvent polarity is critically important for the tautomerization. Most aprotic solvents shift the equilibrium toward the *keto* tautomer by increasing the polarity. The polar protic solvents can form intermolecular hydrogen bonds resulting in a stabilized *keto* form [19–22]; (iv) the planarity of 2-hydroxy species is essential to intramolecular hydrogen bonding and proton transfer reactions [23–25]; (v) last but not least, is the temperature influences on tautomerization and ESIPT efficiency. Several useful papers provide a very insightful investigation of low temperature spectral behavior [26–30]. McDonald and co-authors have investigated a non-fluorescent Schiff base (2′-Hydroxybenzylidene hydrazine carboxylate) in aprotic solvents such as acetonitrile (AcCN) and tetrahydrofuran (THF) at room temperature; however, upon addition of water, an emission at 453 nm related to the ESIPT appeared. By low temperature fluorescence study at −190 °C in AcCN, a strong emission was registered at 521 nm related to the *keto* emission [28]. Hence, tautomerization and ESIPT display cumulative behavior by the abovementioned factors, where by variation of the condition, control over solvent assisted- and photoinduced tautomerization between two switched states could be achieved.

One of the useful features of ESIPT is the possibility to produce both *enol* (N^*) and *keto* (K^*) emission based on the $N^* \leftrightharpoons K^*$ equilibrium in the excited state. Usually, the *keto* emission is characterized by a large Stokes shift [31–33]. A very useful and seminal review by Kwon and Park [11], devoted to ESIPT and its application in materials science, considers different types of molecules and the factors influencing the fundamental photophysical properties. Due to quenching and predominating non-radiative relaxation to the ground state, most of the experimental data indicate that in (polar or nonpolar) solution the quantitative manifestation of the process is characterized by a low fluorescence quantum yield. In contrast, in the solid state, due to J- or H-aggregation, the efficiency can be increased by up to 50–70%, which is one of the reasons for successfully device fabrication such as OLEDs [8,34–36]. Up to now, there are some examples for ESIPT and tautomerization study of the compounds containing fluorophore units with very good performance as sensors and molecular logic gates [10,37,38]. One of the effective fluorophore classes is the 4-aminophthalimide and its aminoalkylated derivatives. They show strong sensitivity upon different solvent environments and are used as fluorescence probes in cell biology, protein labeling as well as fluorescent polymers for flexible OLED's devices. For example, 4-aminophthalimide, having an electron-donating amino group, exhibited a large quantum yield in THF ($\Phi_{fl} = 0.70$), dichloromethane (DCM) ($\Phi_{fl} = 0.76$) and acetone ($\Phi_{fl} = 0.68$), which forms a base to find applicability in materials science [39–41].

Until now, based on analysis of the existing literature, there is scarce information for the synthesis and tautomerism of phthalimide containing 2-hydroxy SB's [42,43]. Therefore, the aim of the current study is to describe the synthesis of two novel 4-substituted phthalimide 2-hydroxy SB's containing salicylic and 2-hydroxy-1-naphthyl parts and to investigate their ground state tautomerism and ESIPT behavior. This is achieved by a combined approach using optical (absorbance and emission) spectroscopy, advanced data processing, DFT calculations and crystallographic analysis. The obtained information could be useful in the design of new tautomeric systems with desired photochemical properties.

2. Experimental

2.1. Materials used

Phthalimide, 2-hydroxy-1-naphthaldehyde, salicylaldehyde, ethyl bromide (EtBr), and trifluoroacetic acid (TFA) were purchased from Sigma-Aldrich and used without further purification. Nitric acid, sulphuric acid, potassium carbonate, *N*,*N*-dimethylformamide (DMF), and methanol (MeOH) were delivered from local supplier Valerus Ltd. For spectroscopy measurements, all solvents were of spectroscopy grade purity.

2.2. Synthesis

The synthetic pathway of the compounds is presented in Scheme 1. To synthesize **1** (4-nitrophthalimide), **2** (4-nitro-N-ethylphtalimide) and **3** (4-amino-N-ethylphthalimide), we have followed the methodology of previously published papers [44,45]. The ^{1}H and ^{13}C NMR spectra of **3** used as an intermediate compound to synthesize 2-hydroxy-Schiff bases are presented in the Supporting information.

2.3. General procedure for the condensation reaction between 4-amino-N-ethylphthalimide and aromatic aldehydes to 2-hydroxy-Schiff bases

N-ethyl-4-aminophthalimide **3** (2.628 mmol, 1.0 equiv) and 2-hydroxy-aromatic aldehydes (2.628 mmol, 1.0 equiv) were suspended in absolute ethanol (EtOH) (25 mL). Subsequently, a catalytic amount of TFA was added (3 drops) and the mixture heated to reflux without stirring for 3–4 h. After cooling to room temperature, the products precipitate and then were filtered off and recrystallized in a minimal amount of EtOH to yield the pure Schiff bases, TLC ($CHCl_3$:EtOAc = 3:2) (Scheme 1). The ^{1}H and ^{13}C NMR spectra are presented in the Supporting information.

2.3.1. Synthesis of the (E)-2-ethyl-5-((2-hydroxybenzylidene)amino) isoindoline-1,3-dione (**4**)

The compound was synthesized as described in the general procedure above from 0.5 g (2.628 mmol) 4-amino-N-ethylphthalimide and 0.321 g/0.275 mL (2.628 mmol) salicylaldehyde, yield 68% as yellow -orange solids, m.p. = 185 °C. ATR-FTIR cm^{-1}: 3443 (ν –OH), 3045 (ν Ar—H), as 2968, s 2930 (ν –CH_3 and > CH_2), s 1762, as 1695 (ν > C= O), 1625 (ν –CH=N-), 1603, 1570, 1492 (ν Ar C=C), as 1400, s 1371 (δ –CH_3 and > CH_2), 1351, 1335 (C-N-C stretching vibration of imide ring). ^{1}H NMR (DMSO-d_6) ppm: 12.45 (1H, s), 9.07 (1H, s), 8.01–7.82 (2H, m), 7.74 (2H, dd, J = 18.4, 7.9 Hz), 7.46 (1H, t, J = 7.8 Hz), 6.99 (2H, p, J = 8.3, 7.9), 3.61 (2H, q, J = 7.0 Hz), 1.17 (3H, t, J = 7.2 Hz). ^{13}C NMR (DMSO-d_6) ppm: 167.80, 167.75, 166.23, 160.77, 134.69, 134.02, 133.16, 128.35, 124.81, 119.89, 119.80, 117.23, 115.82, 32.96, 14.12. MS (ESI+) calculated for $C_{17}H_{14}N_2O_3$, [M^+]: 294.1004; found 294.0996.

2.3.2. Synthesis of the (E)-2-ethyl-5-(((2-hydroxynaphthalen-1-yl)methylene)amino)isoindoline-1,3-dione (**5**)

The compound was synthesized as described in the general procedure above from 0.5 g (2.628 mmol) 4-amino-N-ethylphthalimide and 0.452 g (2.628 mmol) 2-hydroxy-1-naphthaldehyde, yield 71% as red-orange solids, m.p. = 218 °C. ATR-FTIR cm^{-1}: 3447 (ν –OH), 3061 (ν Ar—H), as 2987, s 2942 (ν –CH_3 and > CH_2), s 1762, as 1697 (ν > C= O), 1628 (ν –CH=N-), 1599, 1572, 1479 (ν Ar C=C), as 1470, s 1395 (δ –CH_3 and > CH_2), 1321, 1302 (C-N-C stretching vibration of imide ring). ^{1}H NMR (DMSO-d_6) ppm: 15.37 (1H, s); 9.71 (1H, s); 8.54 (1H, d, J = 8.4 Hz), 8.19 (1H, d, J = 1.7 Hz), 7.93 (1H, d, J = 9.2 Hz), 7.84–7.70 (3H, m), 7.54 (1H, dd, J = 8.4, 8.6 Hz); 7.35 (1H, t, J = 7.4 Hz); 6.98 (1H, d, J = 9.1 Hz); 3.59 (2H, q, J = 7.2 Hz), 1.0.17 (3H, t, J = 7.2 Hz). ^{13}C NMR (DMSO-d_6) ppm: 171.47, 167.65, 167.62, 157.43, 149.92, 138.35, 134.15, 133.51, 129.50, 128.78, 128.72, 127.31, 127.13, 124.75, 124.36, 122.41, 121.35, 114.76, 109.54, 32.92, 14.14. MS (ESI+) calculated for $C_{21}H_{16}N_2O_3$, [M^+]: 344.1161; found: 344.1154.

2.4. Spectral measurements

The NMR spectra were recorded on a Bruker Avance II+ spectrometer operating with frequency 600 MHz for ^{1}H and 125 MHz for ^{13}C in DMSO-d_6. ATR-FTIR spectra of the compounds were recorded on a

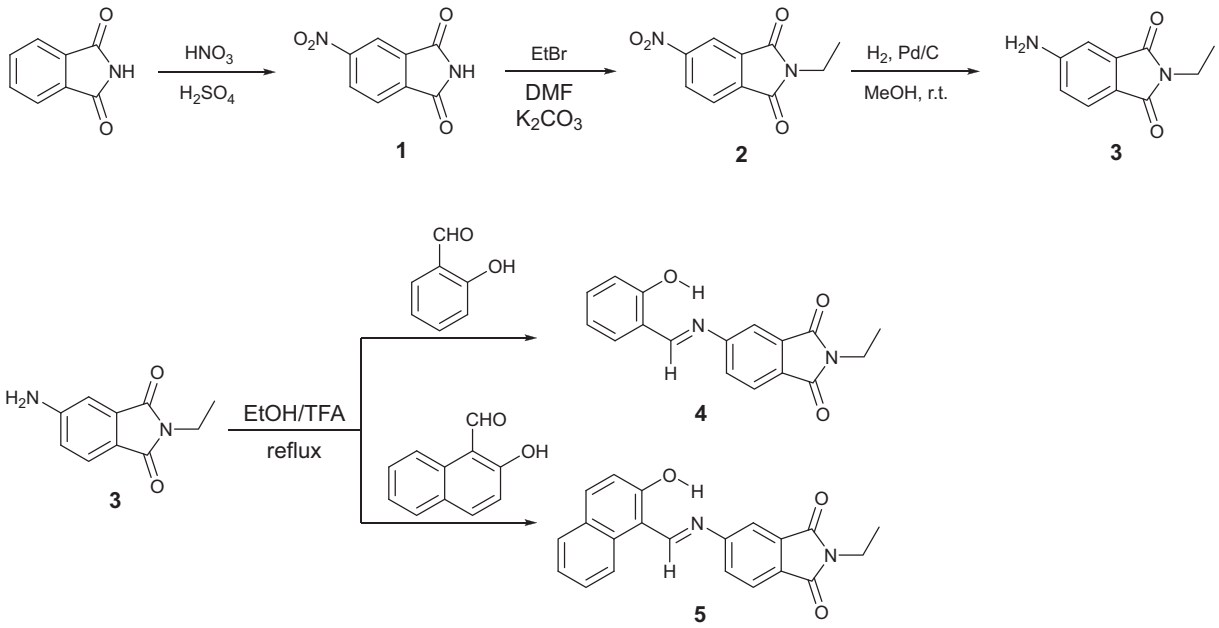

Scheme 1. Synthetic pathway of the 4-substituted phthalimide 2-hydroxy-Schiff bases.

Bruker Tensor 27 FTIR spectrophotometer in the range of 4400–600 cm^{-1} a with resolution of 2 cm^{-1} at room temperature. The external reflection diamond crystal was used and the samples were scanned 128 times. The molecular mass of the compounds was confirmed by a high resolution mass spectrometer Thermo DFS. The UV-VIS spectra were measured on a Jasco V-570 UV–vis–NIR spectrophotometer in spectral grade solvents in the concentration range ~ 10^{-5} mol L^{-1}. The quantitative analysis of the observed *enol⇋ keto* equilibria for **5** was performed by using a Fishing-Net algorithm as described elsewhere [46,47]. The steady-state fluorescence spectra were recorded with a FluoroLog 3–22 (HORIBA) spectrofluorometer in the range 200–800 nm with a resolution of 0.5 nm and double-grating monochromators using as excitation wavelength a value near the absorption maxima of the dyes with concentrations of ~6×10^{-6} mol L^{-1}.

2.5. Quantum chemical calculations

Quantum-chemical calculations were performed using the Gaussian 09 D.01 program suite [48]. The M06-2× functional [49,50] with the TZVP [51] basis set was used for the calculations in the ground and excited state. This fitted hybrid meta-GGA functional with 54% HF exchange was especially developed to describe main-group thermochemistry and non-covalent interactions. The M06-2× functional was selected by a benchmarking procedure, which has shown that there is good empirical relations between the relative stability of the tautomers, defined as ΔE, and the experimentally determined ΔG^o values of set of tautomeric dyes in cycloxexane [52,53]. This qualitative approach shows very good results in predicting the position of tautomeric equilibria for compounds with intramolecular hydrogen bonds as well as describing ground and excited state proton transfer mechanisms [54–58]. Although the computationally ΔG^o values should be preferable, their accuracy is under question even at high level calculations for compounds of the size used in the current study [59,60].

All ground state structures were optimized without restrictions, using tight optimization criteria and an ultrafine grid in the computation of two-electron integrals and their derivatives. The true minima were verified by performing frequency calculations in the corresponding environment.

The implicit solvation was described using the Polarizable Continuum Model (the integral equation formalism variant, IEFPCM, as implemented in Gaussian 09) [61]. The specific effect of methanol was modeled by explicit solvation, keeping the solvent implicitly as well.

The TD-DFT method [62–64] was used for singlet excited state optimizations again without restrictions applying tight optimization criteria and an ultrafine grid in the computation of two-electron integrals and their derivatives.

The transition states were estimated using the STQN method [65] and again verified by performing frequency calculations in the corresponding environment.

2.6. Crystallographic analysis

Single crystals of **4** and **5** were obtained by crystallization from ethanol and acetone, respectively. Suitable crystals were selected and mounted on a MiTeGen holder in oil on a StadiVari diffractometer. Crystals were kept at 200(2) K during data collection. Using Olex2 [66], structures were solved with the ShelXT [67] structure solution program using Intrinsic Phasing and refined with the ShelXL [68] refinement package using least squares minimisation.

Crystal Data for **4**: $C_{17}H_{14}N_2O_3$ (M = 294.30 g/mol): monoclinic, space group $P2_1/c$ (no. 14), a = 9.4560(5) Å, b = 5.0043(2) Å, c = 29.9445(16) Å, β = 98.079(4)°, V = 1402.93(12) $Å^3$, Z = 4, T = 200 (2) K, μ(CuKα) = 0.797 mm^{-1}, *Dcalc* = 1.393 g/cm^3, 14,720 reflections measured (10.442° ≤ 2Θ ≤ 114.396°), 1879 unique (R_{int} = 0.0895, R_{sigma} = 0.0514) which were used in all calculations. The final R_1 was 0.1072 ($I > 2\sigma(I)$) and wR_2 was 0.2903 (all data). **5:** $C_{21}H_{16}N_2O_3$ (M = 344.36 g/mol): monoclinic, space group $P2_1/c$ (no. 14), a = 6.8909(4) Å, b = 14.1083(11) Å, c = 16.8448(10) Å, β = 92.268(5)°, V = 1636.35(19) $Å^3$, Z = 4, T = 200(2) K, μ(CuKα) = 0.772 mm^{-1}, *Dcalc* = 1.398 g/cm^3, 2097 reflections measured (10.512° ≤ 2Θ ≤ 113.8°), 2097 unique (R_{int} = NA, R_{sigma} = 0.0250, BASF: 0.244(11)) which were used in all calculations. The final R_1 was 0.0963 ($I > 2\sigma(I)$) and wR_2 was 0.2857 (all data).

Accession Codes CCDC 1978200–1,978,201 contain the supplementary crystallographic data for this paper. These data can be obtained free of charge via www.ccdc.cam.ac.uk/data_request/cif, or by emailing data_request@ccdc.cam.ac.uk, or by contacting The Cambridge Crystallographic Data Centre, 12 Union Road, Cambridge CB2 1EZ, UK; fax: +441,223 336,033.

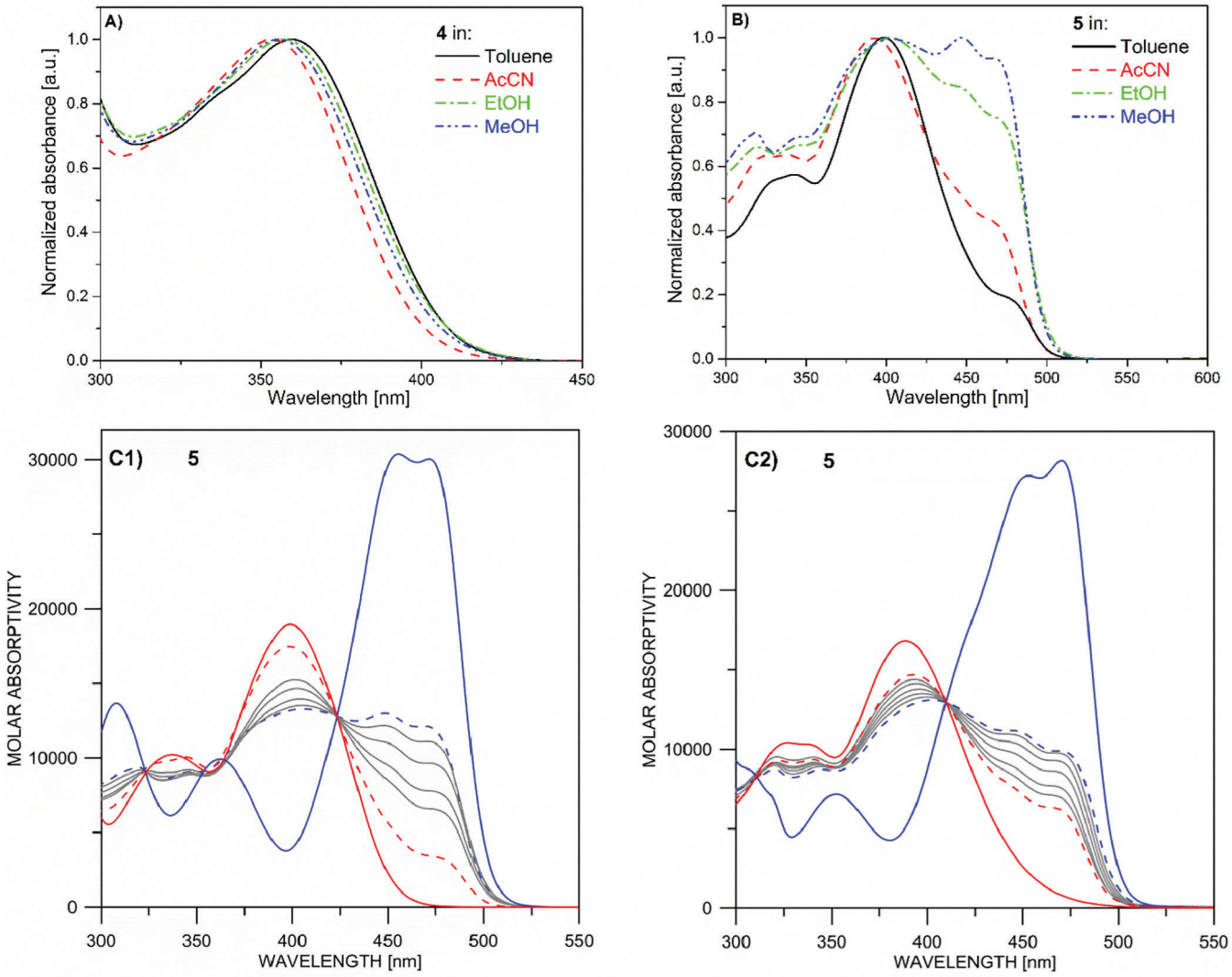

Fig. 1. Absorption spectra of **4** (A) and **5** (B) in toluene, AcCN, EtOH and MeOH. Absorption spectra of **5** (C1) in toluene/MeOH binary solvent mixture from 100% toluene (red dashes) to 100% MeOH (blue dashes) along with the individual spectra of *enol* (red solid line) and *keto* (blue solid line) forms. Absorption spectra of **5** (C2) in AcCN/EtOH binary solvent mixture from 100% AcCN (red dashes) to 100% EtOH (blue dashes) along with the individual spectra of *enol* (red solid line) and *keto* (blue solid line) forms.

3. Results and discussion

3.1. Ground state tautomerism

Two 4-substituted phthalimide 2-hydroxy-Schiff bases containing salicylic and 2-hydroxy-1-naphthyl moieties, respectively, were synthesized via a four steps synthetic procedure (Scheme 1). A classical nitration of phthalimide to 4-nitrophthalimide (**1**) was performed as a first step, followed by a nucleophilic substitution of NH imide by ethyl bromide in DMF in the presence of K_2CO_3 to N-ethyl-4-nitrophthalimide (**2**) [44]. The ethyl group was introduced in order to increases the solubility and to avoid NH deprotonation. Then catalytic hydrogenation of $-NO_2$ to $-NH_2$ by a Pd/C catalyst in MeOH led to N-ethyl-4-aminophthalimide (**3**) and finally, condensation of **3** with salicylic aldehyde or 2-hydroxy-1-naphthaldehyde by refluxing in absolute EtOH in the presence of catalytic amount of TFA yielded 4-substituted phthalimide 2-hydroxy-Schiff bases (**4** and **5**).

Both compounds are potentially tautomeric with a proton transfer proceeding through six-membered intramolecular hydrogen bonding. Hence, from a structural point of view, this bonding and the difference in the 2-hydroxyaryl substituents should influence their tautomerism. As seen from Fig. 1A, the absorption spectra of **4** in nonpolar and polar solvents consist of a single band at ~360 nm and no tautomerism related spectral changes are observed upon changing the solvent. This is expected, because the lack of ground state tautomerism in phenyl derivatives of hydroxyaryl Schiff bases has already been described [3,70]. The low stability of the *keto* tautomer is attributed to the reduced aromaticity in the 2-hydroxyphenyl ring compared to the *enol* form. Compound **5**, containing 2-hydroxy-1-naphthyl moiety, exhibits a major absorbance band around 400 nm in most of the used solvents (Fig. 1B), attributed to the *enol* form in analogy with similar tautomeric Schiff bases [21]. The absorbance of the *keto* tautomer appears as a shoulder around 470 nm, the intensity of which depends on the properties of the solvent (Fig. 1B). The spectra of **5** in binary solvent mixtures are shown in

Table 1
Tautomeric constants[a] and ΔG^o values at room temperature of **5** and **6** in various solvents.

Comp.	Toluene		AcCN		MeOH	
	K_T	ΔG^o kcal mol^{-1}	K_T	ΔG^o kcal mol^{-1}	K_T	ΔG^o kcal mol^{-1}
5	0.12	1.25	0.22	0.90	0.63[b]	0.27
6	0.09[c,d]	1.40	0.56[d]	0.34	0.95[d]	0.03

[a] Defined as *keto*/*enol* ratio;
[b] 0.53 in ethanol;
[c] in cycloexehane;
[d] taken from [21,72].

Table 2
Theoretical prediction of the relative stability of the tautomers of **4**–**6** and some of their structural parameters in the ground state (see also Scheme 2) by using implicit solvation.

Comp	Form	Toluene				MeOH[b,d]			
		ΔE kcal mol^{-1}	R(OH) [Å]	R(NH) [Å]	φ[a] [°]	ΔE kcal mol^{-1}	R(OH) [Å]	R(NH) [Å]	φ[a] [°]
4[c]	**E**	0	0.986	–	−39.3	0	0.989 (0.988)		−39.0 (−35.8)
	TS	8.1	1.361	1.148	−23.1	7.0	1.341	1.161	−25.0
	K	7.3	–	1.038	−15.2	5.8 (5.6)	–	1.035 (1.034)	−18.2 (14.3)
5[c]	**E**	0	0.996	–	−38.0	0	1.000 (0.998)	–	−37.6 (−29.6)
	TS	4.6	1.268	1.201	−24.8	3.9	1.258	1.211	−26.4
	K	2.1	–	1.028	−14.9	1.08 (0.63)	–	1.026 (1.024)	−14.7 (−12.7)
6	**E**	0	0.999	–	−39.9	0	1.003	–	−38.1
	TS	4.2	1.268	1.203	−30.2	3.5	1.253	1.216	−29.5
	K	1.70	–	1.027	−23.6	0.55	–	1.026	−23.4

[a] non-planarity of the phthalimide (in **4** and **5**) or phenyl (in **6**) ring, defined as dihedral angle C(H)-N-C-C;
[b] the results for acetonitrile are the same;
[c] as each of the tautomers of **4** and **5** exists as two possible isomers with respect to the phthalimide part by rotation around the single N—C bond, the most stable isomers (see also Scheme 2) are presented. However, it should be taken into account that the differences in the energies between the isomers of a given tautomer are within 0.3 kcal mol^{-1};
[d] the values using explicit solvation (Fig. 2) are given in brackets.

Fig. 1C1 (toluene/MeOH) and 1C2 (AcCN/EtOH). It is evident that the increase of the volume ratio of alcohol leads to an increase of the amount of the *keto* tautomer. The data from Fig. 1 were processed applying the protocol, earlier developed by us, for quantitative analysis of tautomeric mixtures [47], which yielded the spectra and the molar fractions of the tautomers. The individual spectra are presented on the Fig. 1C1 and 1C2, indicating absorbance at 400 nm for the *enol* form and a structured band in the range 450–500 nm for the *keto* tautomer. The spectral shapes are very similar to the spectra of 1-((phenylimino)methyl)naphthalen-2-ol (**6**), reported before [21]. The advanced chemometric analysis allows, in addition to the individual spectra, an estimation of the molar fractions of the tautomers in each studied solvent and hence, calculation of the tautomeric constants (Table 1).

As seen, the amount of the *keto* tautomer of **5** is fairly low in toluene (11%), while some increase is evident for AcCN (18%) and 40% *keto* form is observed in MeOH. Bearing in mind that the intramolecular hydrogen bonding in Schiff bases is strong enough not to be broken by the solvent [71], the expected effect is related mainly to the polarity of the solvent. Consequently, the tautomeric equilibrium could not be affected by proton acceptor solvents and could be affected by proton donor ones since both tautomeric forms could interact with them. In this respect, the substantial stabilization of the *keto* tautomer, as evident from Figure 1, in alcohols is surprising and needs a deeper consideration. In order to estimate the effect of the phthalimide moiety, a comparative analysis of the new Schiff base **5** and the tautomerism of previously reported **6**, which has been studied in detail [21,31], will be made below.

The theoretical prediction of the relative stability (Table 2 and Scheme 2) of the tautomers of **4**–**6** could be used to clarify the structural and solvent effects. It can immediately be seen that with an energy difference exceeding 5 kcal mol^{-1}, no tautomeric equilibrium is possible in **4** as it is actually observed. Comparison of the relative stabilities of the tautomers of **5** and **6** and their tautomeric constants leads to the conclusion that the replacement of the phenyl ring (**6**) with 4-substituted phthalimide (**5**) leads to destabilization of the *keto* tautomer (increased relative energies in Tables 1 and 2). It could be expected that phthalimide, which contains two carbonyl groups, should act as a strong

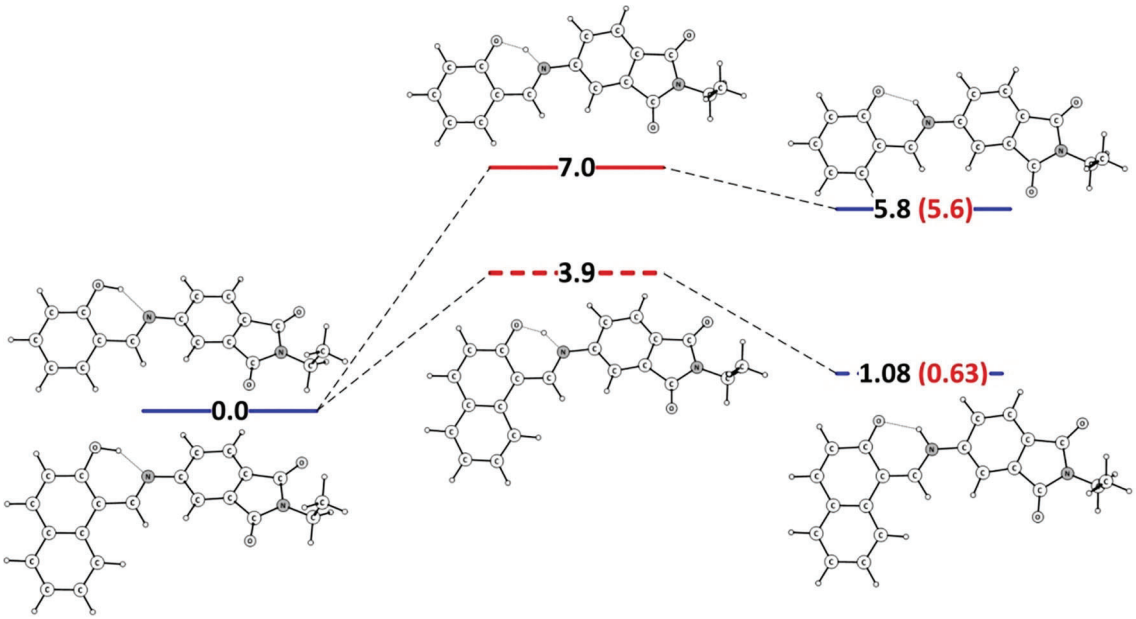

Scheme 2. Sketch of the ground state potential energy surface of **4** and **5** in MeOH using implicit solvation model. The results for explicit solvation in methanol (Fig. 2) are given in red. All values are in kcal mol^{-1} units.

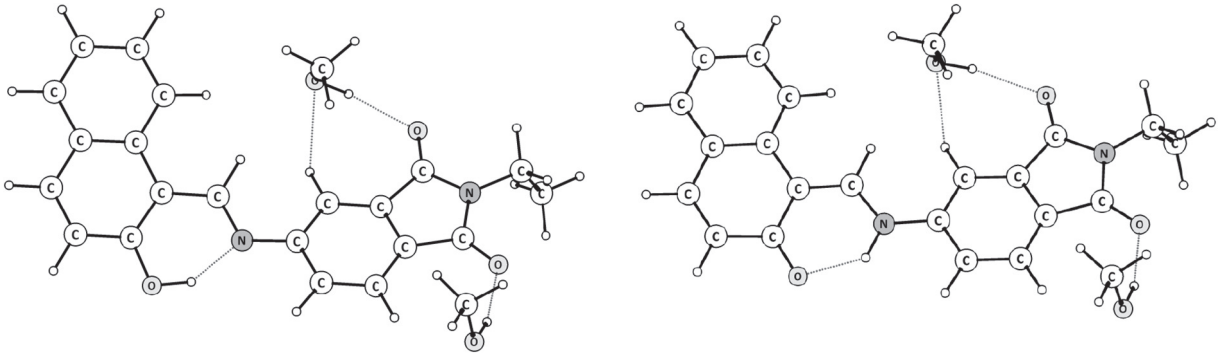

Fig. 2. Model of the methanol – carbonyl group from phthalimide complexes of the *enol* (left) and the *keto* (right) tautomers.

electron-withdrawing group and hence stabilizes preferentially the *keto* tautomer. However, the Schiff bases are non-planar, as also seen in Table 2, and these effects are relatively weak. Analysis of the HOMO and LUMO molecular orbitals of both compounds (Table S1) indicates that the phthalimide moiety provides better charge transfer stabilization in the case of the *enol* form, which could be the explanation of the obtained relative energies. In the case of **6**, there is no substantial difference in the charge transfer in the tautomers, which explains the lack of a straightforward substituent effect on the position of the tautomeric equilibrium, as experimentally proven [21].

The obtained experimental data for the tautomerism of **5** and **6** (Table 1) allow to estimate the reliability of the theoretical predictions. In toluene, the *enol* tautomer is dominating as both theory and experiment suggest. In AcCN, the predicted stability of the *enol* tautomer in both **5** and **6** is overestimated by ~0.2 kcal mol^{-1}, which indicates the reliability of the used theoretical approach. As expected, the change from AcCN to MeOH, using implicit PCM solvation, does not affect the geometry of the tautomers and their stability in terms of quantum-chemical calculations. However, the experiment shows that in MeOH solution, a substantially stronger relative stabilization of the *keto* tautomer is achieved in **5** in comparison with **6**. In **6**, a change in the ΔG^o values from 0.34 (AcCN) to 0.03 (MeOH) kcal mol^{-1} (~ 0.3 kcal mol^{-1} shift) is observed, which is attributed to a better interaction of the carbonyl group of the *keto* tautomer with MeOH, acting as a proton donor solvent in this particular case [71]. In the case of **5**, the change of the solvent leads to a shift of ~0.6 kcal mol^{-1}, which is substantially large. Having in mind that the tautomeric moiety is the same in **5** and **6**, a similar effect of the MeOH should be expected. However, in the case of **5,** there are two additional carbonyl groups in the phthalimide ring that can interact with methanol to provide a long-range indirect stabilization. A simplified model of the complexes of the tautomers with two MeOH molecules is shown on Fig. 2. This specific interaction gives a relative energy of 0.63 kcal mol^{-1} (Scheme 2, the red-colored values) which corresponds, in the frame of the offset discussed above, to the experimental ΔG^o values of 0.27 kcal mol^{-1}. The formation of the complexes with the solvent leads to a decreasing of the nonplanarity of the tautomers (−30° and − 12.7° in *enol* and *keto* forms respectively, see Table 2 for comparison). This kind of indirect solvent assisted stabilization, however, is not able to drastically change the equilibrium when this is not allowed for aromatic reasons, see Scheme 2 in the case of **4**. As seen from Fig. 1B, the quantity of the *keto* tautomer of **5** in MeOH is slightly higher comparing to the other alcohols. Although the alcohols are polar solvents with comparable proton donor and acceptor ability in this particular case (MeOH-tautomer complexes), they can act only as proton donors. Considering the specific solvent parameters, describing the used alcohols in the light of linear solvation energy relationship theory [73–75], the proton donor parameter of MeOH is 0.93, while for the rest of the alcohols it is in the range of 0.79–0.83. This explains reasonably well why the MeOH behaves different in Fig. 1B.

The existence of **4** as a enol tautomer and the stabilization of the keto form in **5** are confirmed by the structures obtained by single crystal X-ray data of both compounds, as shown in Fig. 3. The data clearly indicate the observed effects are native, at least in **4**, and not a result of intermolecular interactions in the crystal. The hydrogen bonds are formed between O9 and N11 with a distance of 2.620(8) Å and an O9-H27…N11 angle of 146.4° for compound **4** and between O11 and N13 with 2.524 (8) Å and an angle of 145.4° for compound **5**. This corresponds to moderate hydrogen bonding [76], explaining why it is so stable.

The non-planarity of **4** is confirmed by the angle formed by the two planes, one containing the phthalimide group and the other one containing the hydroxybenzyl group, of ca. 34°. However, the analogue angle in **5** is quasi planar with an angle of ~1.5°. In terms of packing and intermolecular interactions, compound **4** presents some H-contacts between the hydroxyl group and the carboxyl group of the phthalidime groups of neighboring molecules as well as carbon-carbon interactions between the overlaying hydroxyphenyl groups of two molecules (distance plane to plane: ~3.6 Å). In contrast to **4**, strong interactions exist in compound **5**, where molecules stack along the *a* axis in a head-to-tail fashion and a distance between the planes containing two parallel molecules of ca. 3.4 Å. In this motif, the naphthalene ring is taken in sandwich between two benzene rings of the phthalimide groups.

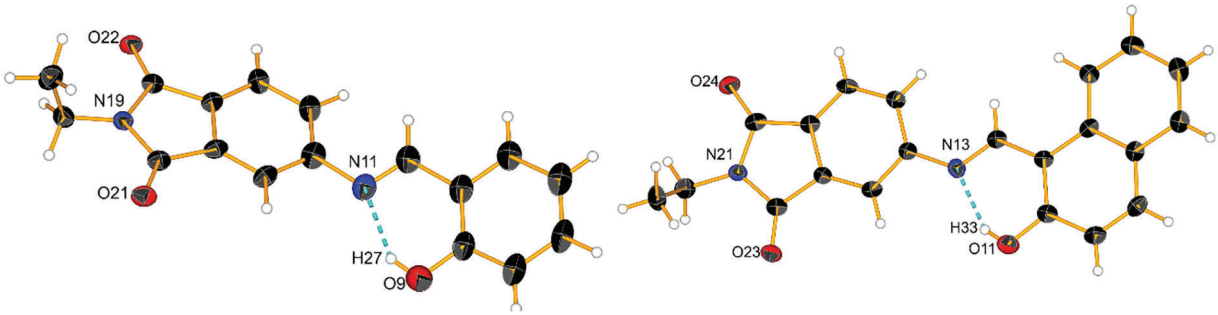

Fig. 3. ORTEP representation of **4** (left) and **5** (right), ellipsoids are drawn with 30% of probability and hydrogen bonds are represented by a blue dashed line.

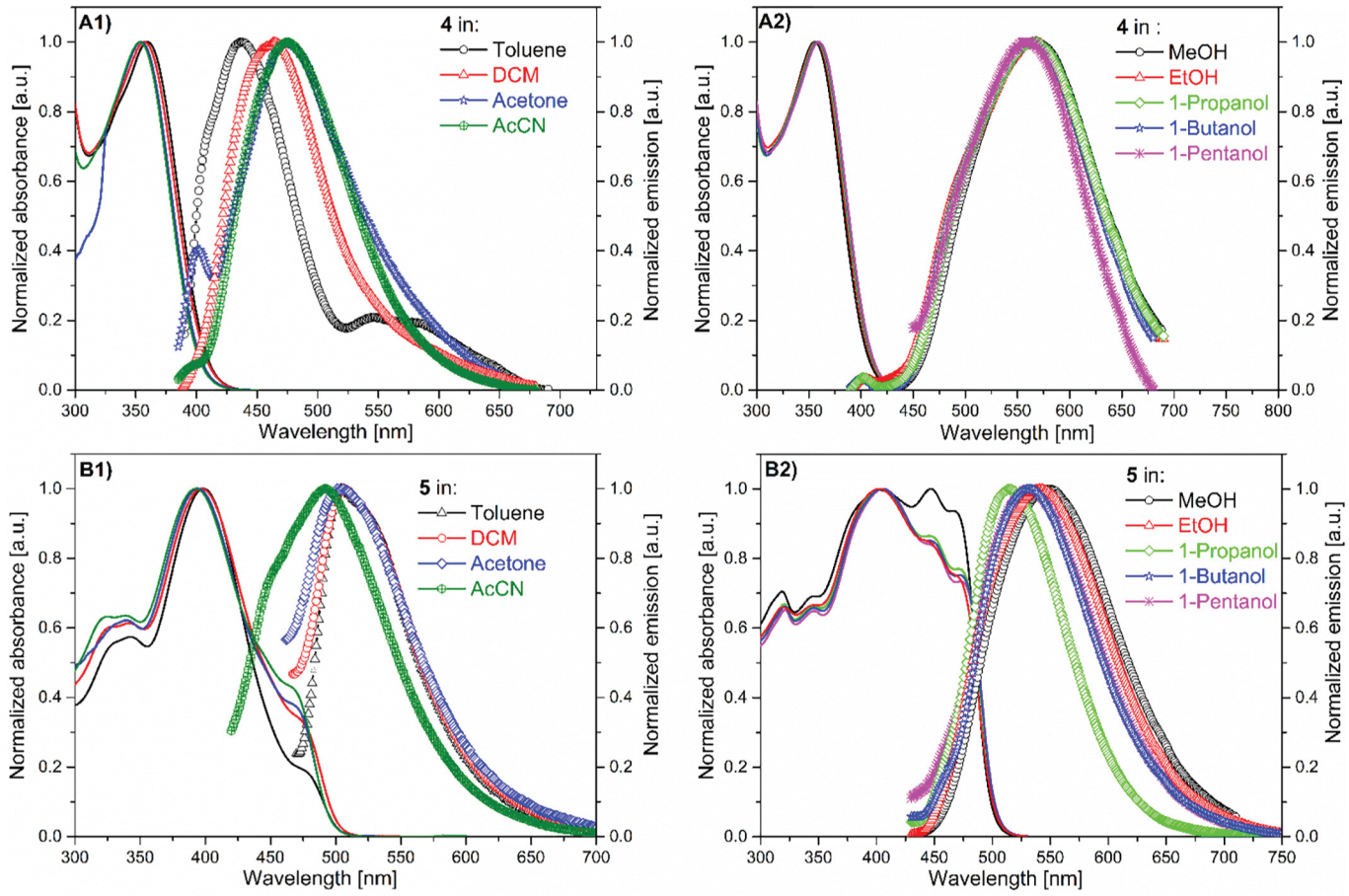

Fig. 4. Experimentally measured absorption and steady-state fluorescence spectra of **4** and **5** in various aprotic solvents (A1 and B1) and different polar alcohols (A2 and B2). The excitation wavelength was set near to the absorption maxima.

Table 3
Summarized results of absorption wavelengths (λ_{abs}), emission wavelengths (λ_{em}), Stokes shifts ($\Delta\bar{\upsilon}$) and efficiency of *enol→keto* conversion (η_{tr}) of the studied 2-hydroxy-Schiff bases in different polarity solvents.

Comp	Solvent	λ_{abs} [nm]	λ_{em} [nm]	Stokes shifts, $\bar{\upsilon}$ [cm^{-1}][a]	η_{tr} [%]
4	Toluene	360	437	4894	–
	DCM	357	464	6459	–
	Acetone	354	474	7151	–
	AcCN	354	474	7151	–
	MeOH	355	566	10,501	–
	EtOH	357	566	10,343	–
	1-Propanol	358	568	10,327	–
	1-Butanol	359	566	10,187	–
	1-Pentanol	359	558	9934	–
5	Toluene	398 478	505	5320	41
	DCM	397 475	507	5460	52
	Acetone	394 470	503	5500	96
	AcCN	393 466	492	5120	100
	MeOH	401 446	548	6690	100
	EtOH	402 447	542	6430	100
	1-Propanol	404 449	514	5300	100
	1-Butanol	405 448	532	5890	100
	1-Pentanol	406 449	533	5870	100

[a] Determined by $\Delta\bar{\upsilon} = 10^7 \times (\frac{1}{\lambda_{abs}} - \frac{1}{\lambda_{em}})$ using long wavelength absorbance band and maximum of the emissions.

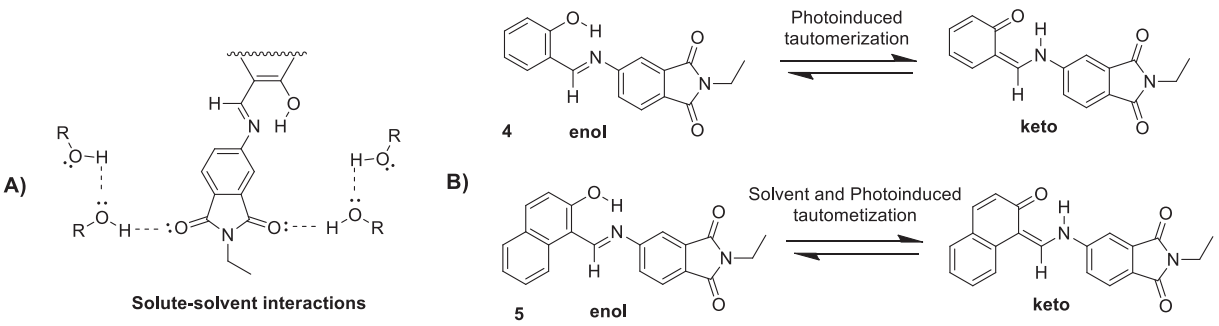

Scheme 3. Specific dye-alcohol interactions with imide carbonyl oxygen by intermolecular hydrogen bonding (A) and tautomerization triggered by a different way (B): photoinduced for **4** and both photoinduced and indirectly solvent assisted for **5**.

The observed results for **5** in solid state are not surprising. The crystal was obtained from acetone, where the enol form is strongly dominating. The strong stacking leads to forced planarization of the molecule and theoretically the sandwich type aggregates could be considered. According to the data from X-ray, two dimer motifs are possible, depending to the mutual position of the N-ethyl groups (see Scheme S1). In both cases the aggregation stabilizes the enol form as it is practically observed in solid state. It should be noted, however, that in the concentration range of UV–Vis spectroscopy not aggregation has been detected in any solvent, but upon evaporation of the solvent it is not excluded.

3.2. Excited state intramolecular proton transfer

Steady-state emissions of **4** display different sensitivity of ESIPT in aprotic solvents (toluene, DCM, Acetone and AcCN), while in protic ones with decreasing polarity (MeOH > EtOH >1-Propanol >1-Butanol >1-Pentanol), the observed emissions are characterized by large Stokes shifts of around 560 nm corresponding to the *keto* tautomer (Fig. 4A1, 4A2 and Table 3). The emission spectra of **5** are characterized by large Stokes shifts that indicate ESIPT and emissions of the *keto* tautomer. All emission bands in the five alcohols ~515–550 nm can be also assigned to the *keto* emission (Fig. 4B1, 4B2 and Table 3).

By setting the excitation wavelength near to the absorption of the *keto* tautomer, we have observed the *keto* emissions (Fig. S8 and S9 in the Supporting information). In all alcohols, the bands match with those obtained after excitation near the *enol* absorption, which confirms that the observed emissions correspond to the *keto* tautomer. The reason is a specific solute-solvent interaction as discussed in the previous section in terms of theoretical calculations, enabling to form intermolecular hydrogen bonding between the carbonyl oxygen of the imide ring and the alcohol (Scheme 3A). This causes additional polarization of the solute, which favors the ESIPT. Krystkowiak and co-authors have studied the fluorescence behaviour of 4-aminophthalimide in various polar solvents [77]. They have observed a large sensitivity and a red-shifted emission in MeOH and EtOH due to the specific solvation by intramolecular hydrogen bonding. The reason for the specific behaviour of the studied SB's is the stability of conjugated base after tautomerization to the *keto* form, which mainly depends on the π-π delocalization between >C=O and aromatic rings and the basicity (nucleophilicity) of –CH=N- nitrogen by the nonbonding electron pair. Obviously, *keto* **5** has a bigger stability due to stronger π-π delocalization of the aromatic naphthalene ring compared to the *keto* **4** with a salicylic moiety. The compounds containing the phthalimide ring can produce aggregate induced emission (AIE) and this can lead to masking of the ESIPT. In order to minimize this effect, we have worked with strongly diluted solutions $C_M \sim 6 \times 10^{-6}$ mol L^{-1}. For comparison, the emissions of **5** at higher concentration $C_M \sim 6 \times 10^{-5}$ mol L^{-1} were measured (Fig. S10 in the Supporting information). At higher concentrations, the red-shifted emissions are observed (506 ÷ 622 nm) in aprotic and protic solvents due to AIE compared to the lower concentration.

The *enol*/*keto* tautomerization can be triggered by solvent or photoexcitation, which is essential to the spatial and temporal control between the two switchable states (Scheme 3B). Moreover, intramolecular photoinduced tautomerization ensures dynamic control of proton transfer reaction in the excited state between both tautomers depending on the solvent environment. For qualitative (or near qualitative) evaluation of the proton transfer in the excited state, we have used a previously described method by us, where the assumption is that in the excited state, the *enol* form undergoes fast transformation to the excited *keto* form and the resulting emission is characterized by large Stokes shifts compared to the *enol* one [31]. We have estimated the relative fraction of the *enol* form by the excitation spectrum, which is

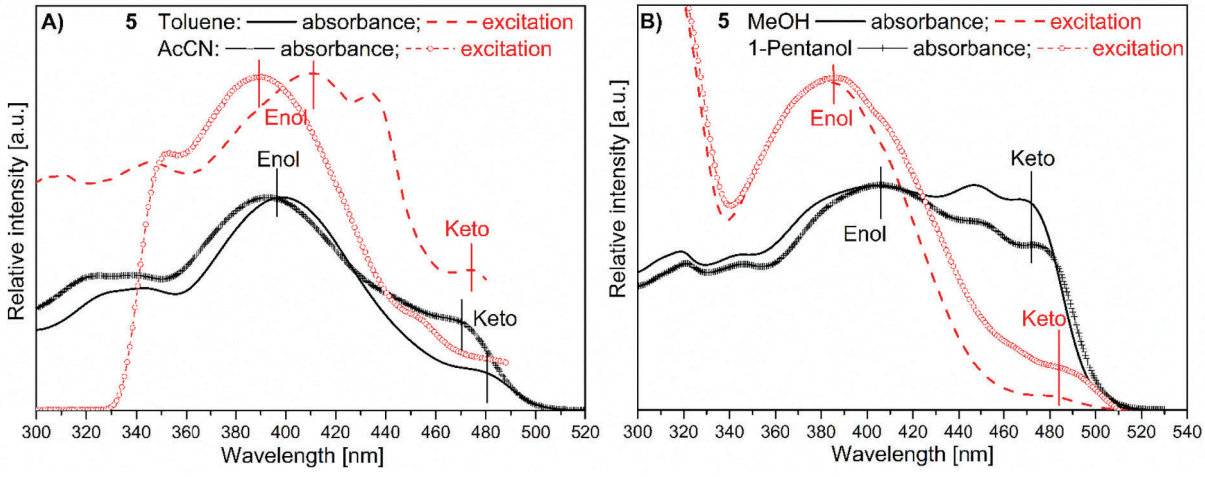

Fig. 5. Absorbance and excitation spectra of **5** in toluene and AcCN (A) as well as in MeOH and 1-Pentanol (B).

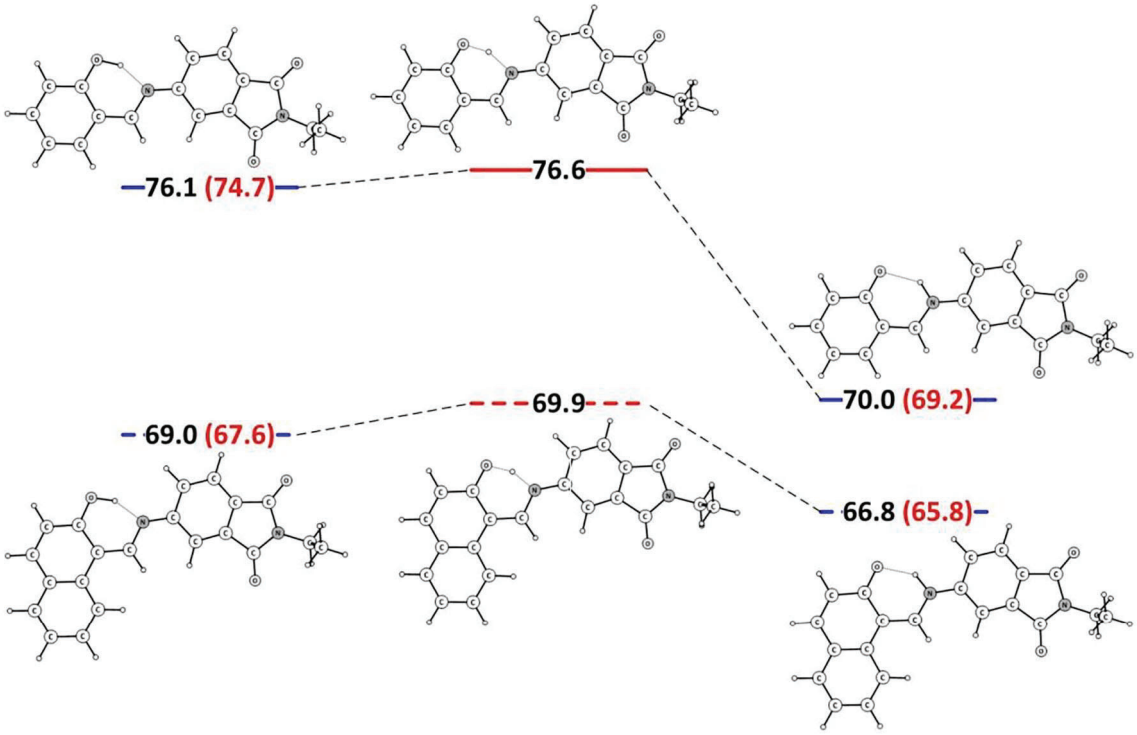

Scheme 4. Sketch of the first singlet exited state potential energy surface of **4** and **5** in MeOH using implicit solvation model. The results from explicit solvation in MeOH (Fig. 3) are red-colored. All values are in kcal mol^{-1} units against the ground state *enol* tautomer (Scheme 2).

converted into the *keto* form through ESIPT. They express the contributions of both forms by the following equations (Eq. (1) and (2)) [31]:

$$I_{exc}(E) = A_E \times Q_K \times \left(\frac{k_{PT}}{k_{PT} + k_d(E)}\right) \quad (1)$$

$$I_{exc}(K) = A_K \times Q_K \quad (2)$$

where A_E and A_K are the absorbance maxima of the *enol* and *keto* forms; $I_{exc}(E)$ and $I_{exc}(K)$ are the excitation intensities at the same wavelengths; k_{PT} is ESIPT rate, $k_d(E)$ is the decay rate and Q_k is the quantum yield of the *keto* form. If the $k_{PT}/k_{PT} + k_d(E)$ is defined as the efficiency of conversion of *enol* into *keto* form η_T, from Eqs. (1) and (2) we can use follows expression (Eq. 3):

$$\eta_T = \frac{I_{exc}(E) \times A_K}{I_{exc}(K) \times A_E} \times 100 \quad (3)$$

Examples of absorbance and excitation spectra in nonpolar and polar aprotic as well as in polar and less polar alcohols are depicted in the Fig. 5. Systemized values of η_T in all used solvents of **5** are available in Table 3. In most aprotic solvents, the compound displays excitation to *keto* tautomer via ESIPT resulting in red-shifted emissions. The highest

Table 4
Theoretical prediction of the relative stability of the tautomers (with respect to the ground state *enol* tautomer) of **4**–**6** and some of their structural parameters in the first singlet excited state (see also Fig. 2 and Scheme 3) by using implicit solvation.

Comp	Form	Toluene				Methanol[b,d]			
		ΔE kcal mol^{-1}	R(OH) [Å]	R(NH) [Å]	φ[a] [°]	ΔE kcal mol^{-1}	R(OH) [Å]	R(NH) [Å]	φ[a] [°]
4[c]	**E**	79.1	1.054	–	−2.3	76.1 (74.7)	1.029 (1.023)	–	−3.6 (−4.4)
	TS	79.2	1.121	1.391	0.0	76.6	1.149	1.348	0.5
	K	73.2	–	1.036	0.9	70.0 (69.2)	–	1.030 (1.031)	1.1 (2.7)
5[c]	**E**	72.3	1.038	–	−3.3	69.0 (67.6)	1.034 (1.028)	–	−3.0 (−4.7)
	TS	73.0	1.193	1.285	0.7	69.6	1.191	1.286	−0.2
	K	70.4	–	1.044	6.6	66.8 (65.8)	–	1.041 (1.039)	1.4 (−4.1)
6	**E**					72.8	1.036	–	6.7
	TS					73.2	1.157	1.327	2.1
	K					68.5	–	1.034	−2.7

[a] non-planarity of the phthalimide (in **4** and **5**) or phenyl (in **6**) ring, defined as dihedral angle C(H)-N-C-C;
[b] the results for acetonitrile are the same;
[c] as each of the tautomers of **4** and **5** exists as two possible isomers with respect to the phthalimide part by rotation around the single N–C bond, here the most stable isomers (see also Scheme 3) are presented;
[d] the values using explicit solvation (Fig. 2) are given in brackets.

rate of conversion up to 100% is observed in all alcohols due to specific solute-solvent interactions.

The theoretical results strongly support this hypothesis (Scheme 4, Table 4). It can be seen that in both compounds, the excited keto tautomer is substantially more stable. Although this is a feature of the 2-hydroxy SB's (strong donor-acceptor stabilization) [79], this could be to some extent attributed also to the planarization of the molecules, which increases the effect of the carbonyl groups from the phthalimide ring. The extent of stabilization of the *keto* tautomer of **4** is substantially larger, which, together with the higher energy of the same tautomer in the ground state, explains the observed larger Stokes shifts.

4. Conclusions

Two new 4-substituted phthalimide 2-hydroxy-Schiff bases (**4** and **5**) have been synthesized and studied by molecular spectroscopy and theoretical calculations. It has been shown that their ground state tautomerism depends on the existing intramolecular hydrogen bonding, the implemented phthalimide moiety and the difference in the 2-hydroxyaryl substituents. In **4**, no tautomeric equilibrium has been observed. In **5**, the tautomeric ratio is determined by the solvent. Comparing spectral properties in acetonitrile and methanol, it has been found that additional indirect solvent stabilization of the *keto* tautomer is achieved in the latter. A simplified theoretical model suggests that the interaction of the methanol molecules with the carbonyl groups in the phthalimide moiety could be responsible for that. Both compounds exhibit excited state intramolecular proton transfer, proven by the large Stokes shifts. The ESIPT barrier in the excited state is fairly low, which leads to the absence of *enol* form emission at the expense of the *keto* emission.

The comparative systematic study of **4** and **5** allow to make following conclusions in terms of structure-property relationship: (i) 2-hydroxy-1-naphthyl moiety of **5** is responsible for indirect solvent-assisted tautomerization in the most aprotic and all protic solvents in the ground state; (ii) compound **4** containing a salicylic moiety does not display tautomerization in the ground state; (iii) both compounds show a high rate of ESIPT in various protic and aprotic solvents; (iv) by variation of the number of condensed phenyl rings in the 2-hydroxyaryl substituents, the control over the ground state and photo-induced tautomerization between two switching states can be achieved.

CRediT authorship contribution statement

Dancho Yordanov: Formal analysis, Investigation.**Vera Deneva:**Formal analysis, Investigation.**Anton Georgiev:**Conceptualization, Methodology, Formal analysis, Writing - original draft.**Aurelien Crochet:** Investigation, Writing - original draft.**Katharina M. Fromm:**Writing - original draft, Supervision.**Liudmil Antonov:**Conceptualization, Methodology, Formal analysis, Writing - original draft, Writing - review & editing, Supervision.

Declaration of competing interest

The authors declare that they have no known competing financial interests or personal relationships that could have appeared to influence the work reported in this paper.

Acknowledgements

This work was financial supported by the Bulgarian National Science Fund under project ДН 18/5 “Novel azo materials and application of their photophysical properties as reversible optical optical storage devices”. Research equipment of distributed research infrastructure INFRAMAT (part of Bulgarian National roadmap for research infrastructures) supported by Bulgarian Ministry of Education and Science under contract D01-284/17.12.2019 was used in this investigation.

Appendix A. Supplementary data

Supplementary data to this article can be found online at https://doi.org/10.1016/j.saa.2020.118416.

References

[1] L. Antonov (Ed.), Tautomerism: Methods and Theories, Wiley-VCH, Weinheim, 2014.
[2] L. Antonov, Tautomerism: Concepts and Applications in Science and Technology, Wiley-VCH Verlag GmbH & Co. KGaA, Weinheim, 2016.
[3] V.I. Minkin, A.V. Tsukanov, A.D. Dubonosov, V.A. Bren, Tautomeric Schiff bases: Iono-, solvato-, thermo- and photochromism, J. Mol. Struct. 998 (2011) 179–191, https://doi.org/10.1016/j.molstruc.2011.05.029.
[4] A. Weller, Uber die Fluoreszenz der Salizylzaure und verwandter Verbindungen, Naturwissenschaften 42 (1955) 175–176, https://doi.org/10.1007/BF00595299.
[5] A.C. Sedgwick, L. Wu, H.-H. Han, S.D. Bull, X.-P. He, T.D. James, J.L. Sessler, B.Z. Tang, H. Tian, J. Yoon, Excited-state intramolecular proton-transfer (ESIPT) based fluorescence sensors and imaging agents, Chem. Soc. Rev. 47 (2018) 8842–8880, https://doi.org/10.1039/C8CS00185E.
[6] X. Xie, G.A. Crespo, G. Mistlberger, E. Bakker, Photocurrent generation based on a light-driven proton pump in an artificial liquid membrane, Nat. Chem. 6 (2014) 202–207, https://doi.org/10.1038/nchem.1858.
[7] H. Yin, H. Li, G. Xia, C. Ruan, Y. Shi, H. Wang, M. Jin, D. Ding, A novel non-fluorescent excited state intramolecular proton transfer phenomenon induced by intramolecular hydrogen bonds: an experimental and theoretical investigation, Sci. Rep. 6 (2016), 19774. https://doi.org/10.1038/srep19774.
[8] V.S. Padalkar, S. Seki, Excited-state intramolecular proton-transfer (ESIPT)-inspired solid state emitters, Chem. Soc. Rev. 45 (2016) 169–202, https://doi.org/10.1039/C5CS00543D.
[9] H. Tian, X. Qiao, Z.-L. Zhang, C.-Z. Xie, Q.-Z. Li, J.-Y. Xu, A high performance 2-hydroxynaphthalene Schiff base fluorescent chemosensor for Al3+ and its applications in imaging of living cells and zebrafish in vivo, Spectrochim. Acta A Mol. Biomol. Spectrosc. 207 (2019) 31–38, https://doi.org/10.1016/j.saa.2018.08.063.
[10] A. Ryabchun, Q. Li, F. Lancia, I. Aprahamian, N. Katsonis, Shape-persistent actuators from Hydrazone Photoswitches, J. Am. Chem. Soc. 141 (2019) 1196–1200, https://doi.org/10.1021/jacs.8b11558.
[11] J.E. Kwon, S.Y. Park, Advanced organic optoelectronic materials: harnessing excited-state Intramolecular proton transfer (ESIPT) process, Adv. Mater. 23 (2011) 3615–3642, https://doi.org/10.1002/adma.201102046.
[12] K.-C. Tang, M.-J. Chang, T.-Y. Lin, H.-A. Pan, T.-C. Fang, K.-Y. Chen, W.-Y. Hung, Y.-H. Hsu, P.-T. Chou, Fine tuning the energetics of excited-state Intramolecular proton transfer (ESIPT): white light generation in a single ESIPT system, J. Am. Chem. Soc. 133 (2011) 17738–17745, https://doi.org/10.1021/ja2062693.
[13] A.I. Said, N.I. Georgiev, V.B. Bojinov, A fluorescent bichromophoric “off-on-off” pH probe as a molecular logic device (half-subtractor and digital comparator) operating by controlled PET and ICT processes, Dyes Pigments 162 (2019) 377–384, https://doi.org/10.1016/j.dyepig.2018.10.030.
[14] M.S. Zakerhamidi, K. Nejati, S. Alidousti, M. Saati, The interactional behaviors and photo-physical properties of azo-salicylaldehyde ligands in solvents media, Spectrochim. Acta A Mol. Biomol. Spectrosc. 150 (2015) 696–703, https://doi.org/10.1016/j.saa.2015.06.015.
[15] M.S. Zakerhamidi, K. Nejati, Sh. Golghasemi Sorkhabi, M. Saati, Substituent and solvent effects on the spectroscopic properties and dipole moments of hydroxyl benzaldehyde azo dye and related Schiff bases, J. Mol. Liq. 180 (2013) 225–234, https://doi.org/10.1016/j.molliq.2013.01.021.
[16] J.M. Fernández-G, F. del Rio-Portilla, B. Quiroz-García, R.A. Toscano, R. Salcedo, The structures of some ortho-hydroxy Schiff base ligands, J. Mol. Struct. 561 (2001) 197–207, https://doi.org/10.1016/S0022-2860(00)00915-7.
[17] H. Ünver, M. Kabak, D.M. Zengin, T.N. Durlu, Keto – enol tautomerism, conformations, and structure, J. Chem. Crystallogr. 31 (2001) 203–209, https://doi.org/10.1023/A:1014395132751.
[18] H. Ünver, K. Polat, M. Uçar, D.M. Zengin, Synthesis and Keto-Enol Tautomerism in N-(2-Hydroxy-1-Naphthylidene)Anils, Spectrosc. Lett. 36 (2003) 287–301, https://doi.org/10.1081/SL-120024579.
[19] P. Nagy, R. Herzfeld, Study of Enol-Keto Tautomerism of N-(2-Hydroxy-1-Naphthylidene)anils, Spectrosc. Lett. 31 (1998) 221–232, https://doi.org/10.1080/00387019808006773.
[20] A. Matwijczuk, D. Karcz, R. Walkowiak, J. Furso, B. Gładyszewska, S. Wybraniec, A. Niewiadomy, G.P. Karwasz, M. Gagoś, Effect of solvent Polarizability on the Keto/Enol equilibrium of selected bioactive molecules from the 1, 3,4-Thiadiazole group with a 2, 4-Hydroxyphenyl function, J. Phys. Chem. A 121 (2017) 1402–1411, https://doi.org/10.1021/acs.jpca.6b08707.
[21] L. Antonov, W.M.F. Fabian, D. Nedeltcheva, F.S. Kamounah, Tautomerism of 2-hydroxynaphthaldehyde Schiff bases, J. Chem. Soc. Perkin Trans. 2 (2000) 1173–1179, https://doi.org/10.1039/b000798f.
[22] W.M.F. Fabian, L. Antonov, D. Nedeltcheva, F.S. Kamounah, P.J. Taylor, Tautomerism in Hydroxynaphthaldehyde Anils and Azo analogues: a combined experimental and computational study, J. Phys. Chem. A 108 (2004) 7603–7612, https://doi.org/10.1021/jp048035z.
[23] Y. Yang, J. Zhao, Y. Li, Theoretical study of the ESIPT process for a new natural product Quercetin, Sci. Rep. 6 (2016), 32152. https://doi.org/10.1038/srep32152.
[24] D. Zheng, M. Zhang, G. Zhao, Combined TDDFT and AIM insights into Photoinduced excited state Intramolecular proton transfer (ESIPT) mechanism in hydroxyl- and

amino-Anthraquinone solution, Sci. Rep. 7 (2017), 13766. https://doi.org/10.1038/s41598-017-14094-5.
[25] D. Yang, G. Yang, J. Zhao, R. Zheng, Y. Wang, J. Lv, A theoretical assignment on excited-state intramolecular proton transfer mechanism for quercetin, J. Phys. Org. Chem. 30 (2017) e 3684, https://doi.org/10.1002/poc.3684.
[26] E. Hadjoudis, I.M. Mavridis, Photochromism and thermochromism of Schiff bases in the solid state: structural aspects, Chem. Soc. Rev. 33 (2004) 579–588 (10.1039. b303644h. doi:10.1039/b303644h).
[27] K. Ogawa, J. Harada, T. Fujiwara, S. Yoshida, Thermochromism of Salicylideneanilines in solution: aggregation-controlled proton Tautomerization, J. Phys. Chem. A 105 (2001) 3425–3427, https://doi.org/10.1021/jp003985f.
[28] L. McDonald, J. Wang, N. Alexander, H. Li, T. Liu, Y. Pang, Origin of water-induced fluorescence turn-on from a Schiff Base compound: AIE or H-bonding promoted ESIPT? J. Phys. Chem. B 120 (2016) 766–772, https://doi.org/10.1021/acs.jpcb.5b10909.
[29] X. Bi, B. Liu, L. McDonald, Y. Pang, Excited-state Intramolecular proton transfer (ESIPT) of fluorescent flavonoid dyes: a close look by low temperature fluorescence, J. Phys. Chem. B 121 (2017) 4981–4986, https://doi.org/10.1021/acs.jpcb.7b01885.
[30] H. Joshi, F.S. Kamounah, G. van der Zwan, C. Gooijer, L. Antonov, Temperature dependent absorption spectroscopy of some tautomeric azo dyes and Schiff bases, J. Chem. Soc. Perkin Trans. 2 (2001) 2303–2308, https://doi.org/10.1039/b106241g.
[31] H. Joshi, F.S. Kamounah, C. Gooijer, G. van der Zwan, L. Antonov, Excited state intramolecular proton transfer in some tautomeric azo dyes and schiff bases containing an intramolecular hydrogen bond, J. Photochem. Photobiol. Chem. 152 (2002) 183–191, https://doi.org/10.1016/S1010-6030(02)00155-7.
[32] M. Ziółek, J. Kubicki, A. Maciejewski, R. Naskręcki, A. Grabowska, Enol-keto tautomerism of aromatic photochromic Schiff base NN′-bis (salicylidene)-p-phenylenediamine: ground state equilibrium and excited state deactivation studied by solvatochromic measurements on ultrafast time scale, J. Chem. Phys. 124 (2006), 124518. https://doi.org/10.1063/1.2179800.
[33] M.A. Satam, R.D. Telore, N. Sekar, Photophysical properties of Schiff's bases from 3-(1, 3-benzothiazol-2-yl)-2-hydroxy naphthalene-1-carbaldehyde, Spectrochim. Acta A Mol. Biomol. Spectrosc. 132 (2014) 678–686, https://doi.org/10.1016/j.saa.2014.05.029.
[34] J. Zhao, S. Ji, Y. Chen, H. Guo, P. Yang, Excited state intramolecular proton transfer (ESIPT): from principal photophysics to the development of new chromophores and applications in fluorescent molecular probes and luminescent materials, Phys. Chem. Chem. Phys. 14 (2012) 8803–8817, https://doi.org/10.1039/C2CP23144A.
[35] H. Xiao, K. Chen, D. Cui, N. Jiang, G. Yin, J. Wang, R. Wang, Two novel aggregation-induced emission active coumarin-based Schiff bases and their applications in cell imaging, New J. Chem. 38 (2014) 2386–2393, https://doi.org/10.1039/C3NJ01557B.
[36] W. Sun, S. Li, R. Hu, Y. Qian, S. Wang, G. Yang, Understanding solvent effects on luminescent properties of a triple fluorescent ESIPT compound and application for white light emission, J. Phys. Chem. A 113 (2009) 5888–5895, https://doi.org/10.1021/jp900688h.
[37] N.I. Georgiev, M.D. Dimitrova, A.M. Asiri, K.A. Alamry, V.B. Bojinov, Synthesis, sensor activity and logic behaviour of a novel bichromophoric system based on rhodamine 6G and 1, 8-naphthalimide, Dyes Pigments 115 (2015) 172–180, https://doi.org/10.1016/j.dyepig.2015.01.001.
[38] J. Jankowska, M.F. Rode, J. Sadlej, A.L. Sobolewski, Excited-state Intramolecular proton transfer: Photoswitching in Salicylidene methylamine derivatives, ChemPhysChem 15 (2014) 1643–1652, https://doi.org/10.1002/cphc.201301205.
[39] R. Orita, M. Franckevičius, A. Vyšniauskas, V. Gulbinas, H. Sugiyama, H. Uekusa, K. Kanosue, R. Ishige, S. Ando, Enhanced fluorescence of phthalimide compounds induced by the incorporation of electron-donating alicyclic amino groups, Phys. Chem. Chem. Phys. 20 (2018) 16033–16044, https://doi.org/10.1039/C8CP01999A.
[40] S.F. Yan, V.N. Belov, M.L. Bossi, S.W. Hell, Switchable fluorescent and Solvatochromic molecular probes based on 4-amino-N-methylphthalimide and a photochromic Diarylethene, Eur. J. Org. Chem. 2008 (2008) 2531–2538, https://doi.org/10.1002/ejoc.200800125.
[41] D. Majhi, S.K. Das, P.K. Sahu, S.M. Pratik, A. Kumar, M. Sarkar, Probing the aggregation behavior of 4-aminophthalimide and 4-(NN-dimethyl) amino-N-methylphthalimide: a combined photophysical, crystallographic, microscopic and theoretical (DFT) study, Phys. Chem. Chem. Phys. 16 (2014), 18349. https://doi.org/10.1039/C4CP01912A.
[42] V. Raditoiu, L. Wagner, A. Raditoiu, P. Ardeleanu, V. Amariutei, A.-A. Sorescu, Schiff bases with Phthalimide residues for Phthalocyanine-azomethine joint Chromogens, Rev. Chim. -Buchar.- Orig. Ed. 60 (2009) 183–188.
[43] H. Yan, K. Zhong, Y. Lu, New Schiff base chromophores composed of salicylaldehyde and naphthalimide derivatives for ion sensor applications, Anal. Methods 11 (2019) 3597–3607, https://doi.org/10.1039/C9AY01035A.
[44] Y. Zhan, X. Zhao, W. Wang, Synthesis of phthalimide disperse dyes and study on the interaction energy, Dyes Pigments 146 (2017) 240–250, https://doi.org/10.1016/j.dyepig.2017.07.013.
[45] K. Chiba, M. Asanuma, M. Ishikawa, Y. Hashimoto, K. Dodo, M. Sodeoka, T. Yamaguchi, Specific fluorescence labeling of target proteins by using a ligand–4-azidophthalimide conjugate, Chem. Commun. 53 (2017) 8751–8754, https://doi.org/10.1039/C7CC03252H.
[46] D. Nedeltcheva, L. Antonov, A. Lycka, B. Damyanova, S. Popov, Chemometric models for quantitative analysis of Tautomeric Schiff bases and Azo dyes, Curr. Org. Chem. 13 (2009) 217–240, https://doi.org/10.2174/138527209787314832.
[47] L. Antonov, Absorption UV-Vis spectroscopy and Chemometrics: From qualitative conclusions to quantitative analysis, in: L. Antonov (Ed.), Tautomerism Methods Theor, Wiley-VCH, Weinheim, Germany 2013, pp. 25–47http://doi.wiley.com/10.1002/9783527658824.ch2. (Accessed 27 May 2016).
[48] M.J. Frisch, G.W. Trucks, H.B. Schlegel, G.E. Scuseria, M.A. Robb, J.R. Cheeseman, G. Scalmani, V. Barone, B. Mennucci, G.A. Petersson, H. Nakatsuji, M. Caricato, X. Li, H.P. Hratchian, A.F. Izmaylov, J. Bloino, G. Zheng, J.L. Sonnenberg, M. Hada, M. Ehara, K. Toyota, R. Fukuda, J. Hasegawa, M. Ishida, T. Nakajima, Y. Honda, O. Kitao, H. Nakai, T. Vreven, J.A. Montgomery Jr., J.E. Peralta, F. Ogliaro, M.J. Bearpark, J. Heyd, E.N. Brothers, K.N. Kudin, V.N. Staroverov, R. Kobayashi, J. Normand, K. Raghavachari, A.P. Rendell, J.C. Burant, S.S. Iyengar, J. Tomasi, M. Cossi, N. Rega, N.J. Millam, M. Klene, J.E. Knox, J.B. Cross, V. Bakken, C. Adamo, J. Jaramillo, R. Gomperts, R.E. Stratmann, O. Yazyev, A.J. Austin, R. Cammi, C. Pomelli, J.W. Ochterski, R.L. Martin, K. Morokuma, V.G. Zakrzewski, G.A. Voth, P. Salvador, J.J. Dannenberg, S. Dapprich, A.D. Daniels, Ã. Farkas, J.B. Foresman, J.V. Ortiz, J. Cioslowski, D.J. Fox, Gaussian 09 Revision D.01, Gaussian, Inc, Wallingford, CT, USA, 2013.
[49] Y. Zhao, D.G. Truhlar, Density Functionals with broad applicability in chemistry, Acc. Chem. Res. 41 (2008) 157–167, https://doi.org/10.1021/ar700111a.
[50] Y. Zhao, D.G. Truhlar, The M06 suite of density functionals for main group thermochemistry, thermochemical kinetics, noncovalent interactions, excited states, and transition elements: two new functionals and systematic testing of four M06-class functionals and 12 other functionals, Theor. Chem. Accounts 120 (2008) 215–241, https://doi.org/10.1007/s00214-007-0310-x.
[51] A. Schäfer, C. Huber, R. Ahlrichs, Fully optimized contracted Gaussian basis sets of triple zeta valence quality for atoms Li to Kr, J. Chem. Phys. 100 (1994) 5829–5835, https://doi.org/10.1063/1.467146.
[52] S. Kawauchi, L. Antonov, Description of the Tautomerism in some Azonaphthols, J. Phys. Org. Chem. 26 (2013) 643–652, https://doi.org/10.1002/poc.3143.
[53] L. Antonov, V. Kurteva, A. Crochet, L. Mirolo, K.M. Fromm, S. Angelova, Tautomerism in 1-phenylazo-4-naphthols: experimental results vs quantum-chemical predictions, Dyes Pigments 92 (2012) 714–723, https://doi.org/10.1016/j.dyepig.2011.06.026.
[54] Y. Manolova, V. Kurteva, L. Antonov, H. Marciniak, S. Lochbrunner, A. Crochet, K.M. Fromm, F.S. Kamounah, P.E. Hansen, 4-Hydroxy-1-naphthaldehydes: proton transfer or deprotonation, Phys. Chem. Chem. Phys. 17 (2015) 10238–10249, https://doi.org/10.1039/C5CP00870K.
[55] Y. Manolova, H. Marciniak, S. Tschierlei, F. Fennel, F.S. Kamounah, S. Lochbrunner, L. Antonov, Solvent control of intramolecular proton transfer: is 4-hydroxy-3-(piperidin-1-ylmethyl)-1-naphthaldehyde a proton crane? Phys. Chem. Chem. Phys. 19 (2017) 7316–7325, https://doi.org/10.1039/C7CP00220C.
[56] S. Hristova, G. Dobrikov, F.S. Kamounah, S. Kawauchi, P.E. Hansen, V. Deneva, D. Nedeltcheva, L. Antonov, 10-Hydroxybenzo[h]quinoline: switching between single- and double-well proton transfer through structural modifications, RSC Adv. 5 (2015) 102495–102507, https://doi.org/10.1039/C5RA20057A.
[57] H. Marciniak, S. Hristova, V. Deneva, F.S. Kamounah, P.E. Hansen, S. Lochbrunner, L. Antonov, Dynamics of excited state proton transfer in nitro substituted 10-hydroxybenzo[h]quinolines, Phys. Chem. Chem. Phys. 19 (2017) 26621–26629, https://doi.org/10.1039/C7CP04476C.
[58] S. Hristova, V. Deneva, M. Pittelkow, A. Crochet, F.S. Kamounah, K.M. Fromm, P.E. Hansen, L. Antonov, A concept for stimulated proton transfer in 1-(phenyldiazenyl)naphthalen-2-ols, Dyes Pigments 156 (2018) 91–99, https://doi.org/10.1016/j.dyepig.2018.03.070.
[59] W.M.F. Fabian, Accurate thermochemistry from quantum chemical calculations? Monatshefte Für Chem. - Chem. Mon. 139 (2008) 309–318, https://doi.org/10.1007/s00706-007-0798-8.
[60] F. Zutterman, O. Louant, G. Mercier, T. Leyssens, B. Champagne, Predicting Keto–Enol equilibrium from combining UV/visible absorption spectroscopy with quantum chemical calculations of Vibronic structures for many excited states. A case study on Salicylideneanilines, J. Phys. Chem. A 122 (2018) 5370–5374, https://doi.org/10.1021/acs.jpca.8b03389.
[61] J. Tomasi, B. Mennucci, R. Cammi, Quantum mechanical continuum solvation models, Chem. Rev. 105 (2005) 2999–3094, https://doi.org/10.1021/cr9904009.
[62] R. Improta, UV-visible absorption and emission energies in condensed phase by PCM/TD-DFT methods, in: V. Barone (Ed.), Comput. Strateg. Spectrosc, John Wiley & Sons, Inc, Hoboken, NJ, USA 2011, pp. 37–75, https://doi.org/10.1002/9781118008720.ch1.
[63] C. Adamo, D. Jacquemin, The calculations of excited-state properties with time-dependent density functional theory, Chem. Soc. Rev. 42 (2013) 845–856, https://doi.org/10.1039/c2cs35394f.
[64] L. Antonov, S. Kawauchi, Y. Okuno, Prediction of the color of dyes by using time-dependent density functional theory, Bulg. Chem. Commun. 46 (2014) 228–237.
[65] C. Peng, P.Y. Ayala, H.B. Schlegel, M.J. Frisch, Using redundant internal coordinates to optimize equilibrium geometries and transition states, J. Comput. Chem. 17 (1996) 49–56, https://doi.org/10.1002/(SICI)1096-987X(19960115)17:1<49::AID-JCC5>3.0.CO;2-0.
[66] O.V. Dolomanov, L.J. Bourhis, R.J. Gildea, J.A.K. Howard, H. Puschmann, *OLEX2*: a complete structure solution, refinement and analysis program, J. Appl. Crystallogr. 42 (2009) 339–341, https://doi.org/10.1107/S0021889808042726.
[67] G.M. Sheldrick, *SHELXT* – integrated space-group and crystal-structure determination, Acta Crystallogr. Sect. Found. Adv. 71 (2015) 3–8, https://doi.org/10.1107/S2053273314026370.
[68] G.M. Sheldrick, Crystal structure refinement with *SHELXL*, Acta Crystallogr. Sect. C Struct. Chem. 71 (2015) 3–8, https://doi.org/10.1107/S2053229614024218.
[70] A. Filarowski, A. Kochel, M. Kluba, F.S. Kamounah, Structural and aromatic aspects of tautomeric equilibrium in hydroxy aryl Schiff bases, J. Phys. Org. Chem. 21 (2008) 939–944, https://doi.org/10.1002/poc.1403.
[71] L. Antonov, W.M.F. Fabian, P.J. Taylor, Tautomerism in some aromatic Schiff bases and related azo compounds: an LSER study, J. Phys. Org. Chem. 18 (2005) 1169–1175, https://doi.org/10.1002/poc.965.

[72] L. Antonov, Tautomerism in Azo and Azomethyne dyes: when and if theory meets experiment, Molecules 24 (2019) 2252, https://doi.org/10.3390/molecules24122252.
[73] M.J. Kamlet, J.L.M. Abboud, R.W. Taft, An examination of linear solvation energy relationships, in: R.W. Taft (Ed.), Prog. Phys. Org. Chem, John Wiley & Sons, Inc, Hoboken, NJ, USA 1981, pp. 485–630http://doi.wiley.com/10.1002/9780470171929.ch6. (Accessed 14 December 2016).
[74] P.J. Taylor, The scope and limitations of LSER in the study of tautomer ratio, in: L. Antonov (Ed.), Tautomerism Methods Theor, Wiley-VCH Verlag GmbH & Co. KGaA, Weinheim, Germany 2013, pp. 277–304, https://doi.org/10.1002/9783527658824.ch11.
[75] C. Reichardt, T. Welton, Solvents and Solvent Effects in Organic Chemistry, Wiley-VCH Verlag GmbH & Co. KGaA, Weinheim, Germany, 2010https://doi.org/10.1002/9783527632220.
[76] T. Steiner, The hydrogen bond in the solid state, Angew. Chem. Int. Ed Engl. 41 (2002) 49–76, https://doi.org/10.1002/1521-3773(20020104)41:1<48::aid-anie48>3.0.co;2-u.
[77] E. Krystkowiak, K. Dobek, A. Maciejewski, Origin of the strong effect of protic solvents on the emission spectra, quantum yield of fluorescence and fluorescence lifetime of 4-aminophthalimide. Role of hydrogen bonds in deactivation of S1-4-aminophthalimide, J. Photochem. Photobiol. Chem. 184 (2006) 250–264, https://doi.org/10.1016/j.jphotochem.2006.04.022.
[79] M. Savarese, É. Brémond, L. Antonov, I. Ciofini, C. Adamo, Computational insights into excited-state proton-transfer reactions in Azo and Azomethine dyes, ChemPhysChem 16 (2015) 3966–3973, https://doi.org/10.1002/cphc.201500589.